Title page

Title: Bleaching and mortality of a photosymbiotic bioeroding sponge under future carbon dioxide emission scenarios

List of authors:

James K.H. Fang[1,2,3], Christine H.L. Schönberg[4], Matheus A. Mello-Athayde[1,2], Michelle Achlatis[1,2], Ove Hoegh-Guldberg[1,2,5], Sophie Dove[1,2]

Affiliations:

[1]Coral Reef Ecosystems Laboratory, School of Biological Sciences, The University of Queensland, St. Lucia, QLD 4072, Australia

[2]Australian Research Council Centre of Excellence for Coral Reef Studies, The University of Queensland, St. Lucia, QLD 4072, Australia

[3]Department of Applied Biology and Chemical Technology, The Hong Kong Polytechnic University, Hung Hom, Kowloon, Hong Kong

[4]School of Earth and Environment and Oceans Institute, The University of Western Australia, Crawley, WA 6009, Australia

[5]Global Change Institute, The University of Queensland, St. Lucia, QLD 4072, Australia

Corresponding author:

James K.H. Fang **(**telephone: + 852 3400 8703, email: james.fang@polyu.edu.hk)

Author contributions:

JKHF, CHLS, OHG and SD conceived and designed the experiment. JKHF, MAMA, OHG and SD performed the experiment. JKHF and CHLS wrote the manuscript with the contribution from MAMA, MA, OHG and SD.

Abstract: The bioeroding sponge *Cliona orientalis* is photosymbiotic with dinoflagellates of the genus *Symbiodinium* and is pervasive on the Great Barrier Reef. We investigated how *C. orientalis* responded to past and future ocean conditions in a simulated community setting. The experiment lasted over an Austral summer under four carbon dioxide emission scenarios: a pre-industrial scenario (PI), a present-day scenario (PD; control) and two future scenarios of combined ocean acidification and ocean warming, i.e. B1 (intermediate) and A1FI (extreme). The four scenarios also simulated natural variability of carbon dioxide partial pressure and temperature in seawater. Responses of *C. orientalis* generally remained similar between the PI and PD treatments. *C. orientalis* under B1 displayed a dramatic increase in lateral tissue extension, but bleached and displayed reduced rates of respiration and photosynthesis. Some B1 sponge replicates died by the end of the experiment. Under A1FI, strong bleaching and subsequent mortality of all *C. orientalis* replicates occurred at an early stage of the experiment. Mortality arrested bioerosion by *C. orientalis* under B1 and A1FI. Overall, the absolute amount of calcium carbonate eroded by *C. orientalis* under B1 or A1FI was similar to that under PI or PD at the end of the experiment. Although bioerosion rates were raised by short-term experimental acidification in previous studies, our findings from the photosymbiotic *C. orientalis* imply that the effects of bioerosion on the reef carbonate budgets may only be temporary if the bioeroders cannot survive long-term in the future oceans.

Keywords: *Cliona orientalis*, *Symbiodinium*, warming, acidification, Great Barrier Reef

Introduction

Bioerosion, here defined as fragmentation or dissolution of calcium carbonate ($CaCO_3$) through biological activities, often represents the counterweight to calcification in the formation of $CaCO_3$-dominated habitats such as coral reefs (e.g. Perry et al. 2008; Schönberg et al. 2017a). Among all bioeroders, sponges of the *Cliona viridis* (Schmidt, 1862) species complex are usually dominant destructive agents on coral reefs, and many of them are widely distributed in warm waters (Schönberg 2002; Calcinai et al. 2007; Schönberg et al. 2017b; van Soest et al. 2017). Like reef-building corals, the success of *C. viridis* complex spp. largely relies on the energy provided by their dinoflagellate symbionts of the genus *Symbiodinium* (e.g. Weisz et al. 2010; Fang et al. 2014). Research interests in bioeroding sponges, particularly in *C. viridis* complex spp. and their interactions with *Symbiodinium*, have dramatically grown over the last decade (e.g. Fang and Schönberg 2015; Schönberg 2017; Schönberg et al. 2017b). Recent studies reported faster sponge bioerosion upon environmental disturbance and natural or experimental acidification (Rützler 2002; Schönberg and Ortiz 2009; Wisshak et al. 2012, 2013, 2014; Fang et al. 2013a; Stubler et al. 2014, 2015; Enochs et al. 2015, 2016; Marulanda-Gómez et al. 2017). As a result, it has become a widely accepted conclusion that sponge bioerosion on coral reefs will likely increase with future ocean acidification (OA) that can impair hard corals (reviewed by Schönberg et al. 2017a). However, Fang et al. (2014) argued that, based on carbon budgets, *C. viridis* complex spp. may be at increasing risk of bleaching (i.e. losing symbiotic *Symbiodinium*) under OA and ocean warming (OW). All these findings suggest that short-term acidification and/or elevated temperature can promote bioerosion by *C. viridis* complex spp., but this enhancement of the sponges' performance may not be sustained under OA and OW, and at some

69 point changed conditions may threaten the survival of the sponges (McElhany 2017; Schönberg
70 et al. 2017a).
71
72 The present study aimed to test the likelihood of bleaching and mortality of a sponge species in
73 the *C. viridis* species complex under combined OA and OW using a simulated community
74 setting, which was more environmentally realistic compared to other studies in the same context.
75 We chose an Indo-Pacific species, *Cliona orientalis* Thiele, 1900, which is pervasive on the
76 Australian Great Barrier Reef (GBR) and has been widely used as a model species in bioerosion
77 studies (e.g. Schönberg and Wilkinson 2001; Wisshak et al. 2012, 2013; Fang et al. 2013a, 2014,
78 2016). The experiment on *C. orientalis* was done in replicated mesocosms as described by Dove
79 et al. (2013). Dove and co-workers built replicas of local benthic communities on the southern
80 GBR and applied various scenarios of partial pressure of carbon dioxide (pCO_2) and temperature
81 while preserving the natural variability of the two factors. The experiment on *C. orientalis* lasted
82 over an Austral summer (late September 2011 to early February 2012) that included a
83 progressive acclimation period (1.5 months) followed by a full exposure period (3 months) under
84 four CO_2 emission scenarios: a preindustrial scenario (PI), a present-day scenario (PD; control)
85 and two future scenarios of combined OA and OW, including an intermediate scenario B1,
86 equivalent to the Representative Concentration Pathway 4.5 (RCP4.5), and an extreme scenario
87 A1FI, equivalent to RCP8.5 (Rogelj et al. 2012). This is, to our knowledge, the first experiment
88 on any bioeroding sponge in a simulated community setting under the combined effects of pCO_2
89 and temperature.
90

In our earlier study during an Austral spring and early summer, *C. orientalis* displayed distinctly increased growth and bioerosion rates under B1 and A1FI, but late in the experiment *C. orientalis* completely bleached under A1FI conditions (99.5% loss of *Symbiodinium*; Fang et al. 2013a). As the experiment of Fang et al. (2013a) was terminated at the time of bleaching, we were unable to provide further insights into survival, recovery or sub-lethal consequences in the bleached sponge. Using an extended experimental period under the same scenarios, the present work sought answers to the following questions: Would *C. orientalis* be able to maintain high rates of growth and bioerosion at the height of summer under B1 and A1FI? Would *C. orientalis* bleach during the summer under other scenarios apart from the extreme A1FI? Would bleached *C. orientalis* be able to recover and survive? By answering these questions, we can provide a more complete outlook into the possible consequences of sponge bioerosion on the carbonate budgets of future coral reef ecosystems. The present work did not attempt to separate the individual effects of pCO_2 and temperature on *C. orientalis*, but assessed the sponge responses to more realistic CO_2 emission scenarios by combining OA and OW, two factors that are concurrently altered by anthropogenic emissions of CO_2 (Meehl et al. 2007). The independent roles of pCO_2 and temperature in the ecophysiology of *C. orientalis* have been investigated by Achlatis et al. (2017).

Materials and methods

Collection and preparation of experimental cores

All biological materials were collected from 5 m depth at Harry's Bommie, a reef slope habitat off Heron Island on the southern GBR that also served as the reference site for our environmental parameters (23°27' S; 151°55' E; see Dove et al. 2013). Cores of *C. orientalis* were collected

from ten colonies of sponge-invaded massive coral *Porites* sp. Two sizes of cores, approximately 35 mm and 20 mm in diameter, were obtained using a pneumatic drill fitted with corresponding hole-saws. Collected cores from all colonies were mixed and randomly used in the experiment. The larger cores (35 mm) were freshly horizontally cut into two parts at Heron Island Research Station. The top parts were approximately 8 mm in height and were fully penetrated by *C. orientalis*. These sponge-penetrated cores were maintained in flow-through natural seawater for one week, allowing them to heal before being used in the experiment as sponge cores. The bottom parts of the larger cores were further cut to approximately 10 mm in height to remove all remaining *C. orientalis* tissue and to produce skeletal cores of massive *Porites*, which were then cleaned in 12.5% sodium hypochlorite and thoroughly rinsed in Milli-Q water (Merck Millipore, Australia). The cleaned skeletal cores were dried at 60 °C, weighed and reconditioned in flow-through natural seawater for three days, serving as initially bioeroder-free cores of $CaCO_3$ (blank cores). The smaller cores (20 mm) of *C. orientalis* were cut and treated in the same way as the larger ones. After the healing period, the smaller, fully sponge-penetrated top parts were tied as grafts onto some of the blank cores to produce the third type of experimental cores (mixed cores; Fig. 1).

The cores were divided into four groups, each containing nine sponge cores, nine mixed cores and nine blank cores. Each group was acclimated to one of the four scenario treatments (see below) in three flow-through aquaria over 1.5 months by progressive exposure to 0%, 20%, 40%, 60%, 80% and 100% treatment seawater mixed with 100%, 80%, 60%, 40%, 20% and 0% natural seawater, respectively. The acclimated cores were then transferred into the replicate mesocosms for each corresponding treatment (3 replicate cores × 3 core types × 3 replicate

mesocosm tanks × 4 treatments). The three types of cores had different uses within the experiment. The sponge cores putatively excluded the occurrence of other organisms that would confound the results. These cores were used to determine chlorophyll fluorescence of *Symbiodinium in hospite*, as well as net rates of respiration and photosynthesis by the holobiont. However, in the sponge cores there was no blank substrate for *C. orientalis* to extend into. Therefore, growth and bioerosion capability of *C. orientalis* were measured in the mixed cores, which provided the sponge grafts with a large underlying substrate of blank $CaCO_3$. Any change in $CaCO_3$ mass in the underlying substrate of the mixed cores represented a net change due to bioerosion by *C. orientalis*, bioerosion and calcification by other organisms, as well as different extents of $CaCO_3$ dissolution in different treatments. In this regard, the blank cores were used to determine the net changes in $CaCO_3$ mass unrelated to *C. orientalis*, and to provide correction factors for sponge bioerosion data obtained from the mixed cores in the four treatments. It should be noted that the blank cores had no top cores attached and thus larger areas of exposed substrate compared to the sponge cores. Therefore, corrections against the blank cores may have resulted in an underestimation of the sponge bioerosion in the sponge cores. Nevertheless, the influence of other organisms on our results appeared to be not significant given the low biomass determined in the blank cores (3.26% ± 0.04%).

Reconstruction of local reef communities in mesocosms

Our experiment was conducted in replicated mesocosms at Heron Island Research Station that were described in more detail by Dove et al. (2013). Typical reef organisms, sediments and rocks were collected from the reference site and placed into twelve outdoor flow-through circular tanks as the mesocosms (300 L each). The reef communities within the mesocosms were acclimated to

160 the treatment conditions (see below) by slowly increasing the relative proportions of treatment
161 seawater to natural seawater over 2.5 months prior to the full exposure period, which started in
162 early November. At this point, the three types of acclimated cores (sponge cores, mixed cores
163 and blank cores) were introduced into the mesocosms. The percentage cover of *C. orientalis* (in
164 the sponge cores and mixed cores) was about 1% of the simulated communities, which was
165 comparable to the natural abundances of *C. orientalis* on the GBR (as calculated from relative
166 values in Schönberg 2001). The mesocosm communities also comprised eight species of hard
167 corals (35% cover), dead coral skeletons, sediments and crustose calcareous algae (48% cover),
168 macroalgae (15% cover), and motile invertebrates such as herbivorous snails and sea cucumbers
169 (1−2% cover), as well as herbivorous fish (see Table 1 in Dove et al. 2013). The mesocosms
170 were covered by light filters (Marine Blue #131, Lee Filters, UK) to generate light conditions
171 similar to those at the 5 m reference site (500−600 µmol photons m^{-2} s^{-1} at noon; Dove et al.
172 2013; Sampayo et al. 2016). Circulation was enhanced by one dual-blower wave-maker per
173 mesocosm (JVP 12000L/H, ProAqua, Australia).
174
175 ***Simulation of four CO_2 emission scenarios***
176 Treatment seawater was supplied by a computer-controlled pCO_2 and temperature simulation
177 system (see Dove et al. 2013). In brief, seawater was continuously pumped from the reef flat of
178 Heron Island through a sand filter (10 µm) into four mixing sumps (> 8000 L each), in which the
179 system simulated the PI, B1 and A1FI scenarios by applying past and future divergences as
180 offsets to the PD conditions of seawater pCO_2 and temperature monitored at Harry's Bommie
181 (raw data available online at www.pmel.noaa.gov/co2/story/Heron+Island). Treatment seawater
182 in the four mixing sumps, one sump per treatment (PI, PD, B1 or A1FI), was supplied via a flow-

183 through system to the twelve mesocosms (3 replicate tanks × 4 treatments). The experiment was
184 exposed to the full scenario conditions from early November 2011 to early February 2012.
185 During this period of Austral summer, pCO_2 in treatment seawater remained relatively constant
186 and was determined to be 301 ± 11 µatm under PI, 405 ± 25 µatm under PD, 611 ± 17 µatm
187 under B1, and 1009 ± 8 µatm under A1FI (mean ± standard error of the mean, SEM). Daily
188 average temperatures increased from 23.6 to 26.7 °C under PI, 24.5 to 27.7 °C under PD, 26.7 to
189 30.1 °C under B1, and 28.4 to 31.4 °C under A1FI in treatment seawater during the same period.
190 These data of pCO_2 and temperature along with other parameters of seawater chemistry in the
191 experiment were previously reported (see Fig. 1 and Table S1 in Dove et al. 2013).
192
193 Unexpected bleaching of some *C. orientalis* cores and some corals occurred in the PD treatment
194 (control) during the last two weeks of the experiment, when seawater temperatures exceeded the
195 maximum monthly mean (MMM). Dove et al. (2013) monitored the health of these organisms
196 and provided respective background data. In the present study, biological data of *C. orientalis*
197 and its *Symbiodinium* were obtained from the sponge cores (light harvesting efficiency and
198 oxygen flux) and from the mixed cores (lateral tissue extension) in mid January, i.e. about a
199 week before the PD bleaching and at a time when all cores of *C. orientalis* bleached in B1 and
200 died in A1FI (see Results). The experiment was terminated in early February, after which $CaCO_3$
201 mass was quantified for the lower substrate parts of the mixed cores and for the blank cores to
202 elucidate the impact of *C. orientalis* on the reef carbonate budgets when subjected to different
203 extents of bleaching and mortality affected by the four scenarios.
204
205 ***Light harvesting efficiency of Symbiodinium within the sponge cores***

Light harvesting efficiency of photosystem II has been determined in *Symbiodinium* in sponges and corals upon thermal stress (e.g. Jones et al. 1998; Wisshak et al. 2013). It was measured here for *C. orientalis* under the four CO_2 emission scenarios using a pulse-amplitude modulated chlorophyll fluorometer (Maxi Imaging-PAM, Walz, Germany). After a dark acclimation period for 1 h during daytime, the sponge cores were assessed on the top surface for three photochemical parameters including apparent absorptivity (Abs), minimum fluorescence yield (F_o) and maximum quantum yield of photosystem II (F_v/F_m) following Fang et al. (2016). Abs and F_o estimated the relative amount of *Symbiodinium* in *C. orientalis*, while F_v/F_m represented the relative efficiency of *Symbiodinium* to process captured photons for photosynthesis. All three variables (Abs, F_o and F_v/F_m) are dimensionless.

Oxygen flux of the sponge cores

The sponge cores were individually incubated in sealed clear acrylic chambers (250 mL each), which were equipped with magnetic stirrers and maintained at the corresponding treatment temperatures. Seawater used in the incubation was provided directly from the respective treatments after being filtered through 0.45 µm (Merck Millipore). The sponge cores were exposed to darkness (0 µmol photons m^{-2} s^{-1}) for 20 min, then to a saturating light intensity (600 µmol photons m^{-2} s^{-1}) for 20 min, and to darkness again for the last 10 min. Seawater oxygen levels during the incubation were continuously logged using optical dipping probes connected to an OXY-10 meter (PreSens, Germany). Rates of dark respiration (DR) and maximum net photosynthesis (NP_{Max}) in the sponge cores were indicated by the decrease and increase in seawater oxygen levels over the first and second 20 min, respectively. The further decrease in oxygen level over the last 10 min was used to determine light-enhanced dark respiration (LEDR),

which was an estimate of light respiration that could not be measured in the presence of photosynthesis in the light (Middlebrook et al. 2012; Fang et al. 2014). DR, LEDR and NP_{Max} were expressed as net oxygen production rates per unit sponge top surface area (μg O_2 cm^{-2} h^{-1}).

It should be noted that treatment seawater may have been re-filtered through the sponge during the 50-min incubation, according to the pumping rates of *C. orientalis* estimated from the inshore central GBR (on average 0.22 mL s^{-1}, open oscula; Table 1 in Strehlow et al. 2016). Nevertheless, this potential re-filtration did not appear to have any influence on our results, given that each rate of oxygen was a slope calculated from 40 (for DR and NP_{Max}) or 20 time-series data points (for LEDR; Fig. 3) and most slopes achieved very high r^2 values in linear regression (> 0.95). This linear response of *C. orientalis* to consume and produce oxygen suggests generally undisturbed conditions of the sponge throughout the incubation period.

Sponge lateral tissue extension on the mixed cores

All experimental cores were photographed on the top surface using a Lumix DMC-TS3 waterproof camera (Panasonic, Japan) in the morning after the oxygen flux assay. Areas of *C. orientalis* tissue on the cores were estimated from these photographs using Coral Point Count with Excel extensions 4.0 (Kohler and Gill 2006). Surface growth of *C. orientalis* was quantified as lateral tissue extension beyond the original graft areas onto the bottom substrate of the mixed cores (mm^2). Obtained values were used to assess relative growth of *C. orientalis* among the treatment scenarios.

$CaCO_3$ mass in the blank cores and mixed cores

252 The blank cores were used to quantify net mass changes in $CaCO_3$ unrelated to *C. orientalis*.
253 After the experiment, all cable ties were removed. The blank cores were rinsed in Milli-Q water,
254 dried at 60 °C, and then individually placed in pre-weighed crucibles and combusted at 550 °C to
255 remove organic matter. Remaining ash (inorganic materials) in the crucibles was cooled down to
256 room temperature in a desiccator, weighed and further combusted at 950 °C to evolve CO_2 from
257 $CaCO_3$. Remaining ash (mostly calcium oxide at this stage) was cooled down and weighed again.
258 The lost weight in the inorganic materials from 550 °C to 950 °C represented the amount of CO_2
259 being evolved, which was used to calculate the weight of $CaCO_3$ in each blank core according to
260 the molecular mass ratio of CO_2 to $CaCO_3$ (Fang et al. 2013b). This yielded the final $CaCO_3$
261 weight at the end of the experiment. The initial weight of $CaCO_3$ in each blank core was
262 estimated from the core's initial dry weight. To produce a conversion factor between $CaCO_3$
263 weight and dry weight, nine extra skeletal fragments of massive *Porites* were cleaned, dried and
264 weighed, and were then combusted at 550 °C and 950 °C to determine $CaCO_3$ weight as
265 described above. From these extra fragments, the ratio of $CaCO_3$ weight to dry weight was found
266 to be 0.97 ± 0.01 (mean ± SEM). This mean value was used as the conversion factor. Net loss of
267 $CaCO_3$ in the blank cores during the experiment (final weight – initial weight) was expressed as
268 a percentage of initial weight.
269
270 The mixed cores were used to estimate the extent of bioerosion by *C. orientalis* over the whole
271 experimental period. The upper sponge grafts and cable ties were removed from the mixed cores,
272 while the lower substrate parts were used to determine the difference between initial and final
273 weights of $CaCO_3$ in the same way as for the blank cores. As we did not assess the sponge tissue
274 areas underneath the grafts that had invaded the lower substrate in the mixed cores, the resulting

bioerosion data were simply corrected for the percentage net changes in $CaCO_3$ mass estimated from the blank cores and were expressed as the absolute loss of $CaCO_3$ associated with *C. orientalis* (g).

Statistical analysis

Nine parameters including Abs, F_o, F_v/F_m, DR, LEDR, NP_{Max} and lateral tissue extension by *C. orientalis*, as well as the changes in $CaCO_3$ mass when the sponge grafts were present (the mixed cores) and absent (the blank cores), were compared among the scenario treatments using nested analysis of variance (nested ANOVA; n = 9, of which 3 cores × 3 tanks per treatment). As *C. orientalis* died in the A1FI treatment (see Results), most comparisons in the nested ANOVA contained only PI, PD and B1, except for the two parameters of $CaCO_3$ mass that were compared among four treatments. Most datasets failed to meet the assumptions of data normality and homogeneity of variance, even after common data transformations (e.g. logarithmic, square-root and cube). Therefore, all datasets were consistently rank-transformed prior to the nested ANOVA. Statistical procedures were carried out using the software Statistica v11 (StatSoft, USA).

Results

The sponge cores, mixed cores and blank cores were regularly observed during the summer period under the four scenarios in the mesocosms. Turf algae grew on the coral substrate and cable ties, but were cropped regularly by herbivores living within the mesocosms. Crustose calcareous algae were also found on the coral substrate and cable ties, and their abundance appeared to be higher under the PI and PD conditions compared to B1 and A1FI, but was not

298 further quantified (Fig. 1). Sea cucumbers were occasionally found in close vicinity of *C.*
299 *orientalis* in all treatments. Apart from this, no clear interactions between *C. orientalis* and other
300 mesocosm organisms were observed under all scenarios regardless of day or night. The colour of
301 *C. orientalis* tissue changed diurnally, appearing dark brown in the morning and mid-day but
302 becoming paler in the late afternoon and at night.
303
304 *C. orientalis* displayed different timing and severity of bleaching and mortality depending on the
305 treatment scenarios, with the earliest bleaching being observed in A1FI. All individuals of A1FI
306 *C. orientalis* bleached in late November when A1FI temperatures attained ~2 °C above the
307 MMM specific to the reference site (see Table 1 in Dove et al. 2013). A1FI *C. orientalis* died in
308 all sponge cores and mixed cores within a month of bleaching. The remaining substrate that had
309 previously been inhabited by *C. orientalis* in A1FI was full of boreholes, brittle and rapidly
310 occupied by turf algae (Fig. 1). Under B1, lateral tissue growth of *C. orientalis* was prominent
311 and fast. However, all sponge cores and mixed cores of B1 *C. orientalis* bleached by early
312 January when B1 temperatures reached ~2 °C above the site-specific MMM (Fig. 1). A third of
313 the bleached cores of B1 *C. orientalis* died. Under PD, some cores of *C. orientalis* also bleached
314 at the height of summer in late January when natural temperatures exceeded the site-specific
315 MMM. All bleached and unbleached PD *C. orientalis* survived until the end of the experiment in
316 early February. Under PI, *C. orientalis* did not bleach and no mortality occurred during the
317 experiment.
318
319 Chlorophyll fluorescence and oxygen fluxes of the sponge cores were measured in mid January
320 and were compared across PI, PD and B1, at which time all sponge cores survived in these three

321 treatments. The sponge mortality in A1FI precluded such measurements. The mean values of
322 Abs, F_o and F_v/F_m describing the relative chlorophyll content and photochemical capability of
323 *Symbiodinum* in *C. orientalis* all remained similar between PI (0.70, 0.14 and 0.39, respectively)
324 and PD (0.72, 0.14 and 0.41, respectively; Fig. 2, Table 1). However, Abs and F_o significantly
325 decreased to near zero and F_v/F_m significantly dropped by >70% in bleached *C. orientalis* under
326 B1 (0.00, 0.04 and 0.10, respectively). Similar patterns were observed for oxygen fluxes of the *C.*
327 *orientalis* holobiont in terms of DR, LEDR and NP_{Max}, which were expressed as net oxygen
328 production rates (Fig. 3). The absolute mean values of DR and LEDR were significantly reduced
329 to about half under B1 (−22.6 and −34.3 µg O_2 cm^{-2} h^{-1}, respectively) compared to PI (−51.2 and
330 −69.0 µg O_2 cm^{-2} h^{-1}, respectively) and PD (−53.3 and −61.3 µg O_2 cm^{-2} h^{-1}, respectively).
331 Moreover, NP_{Max} under B1 (7.54 µg O_2 cm^{-2} h^{-1}) significantly decreased by >90% compared to
332 PI (104.3 µg O_2 cm^{-2} h^{-1}) and PD (93.3 µg O_2 cm^{-2} h^{-1}; Fig 3, Table 1).
333
334 Surface tissue growth on the mixed cores was compared among surviving *C. orientalis* under PI,
335 PD and B1 in mid January. Due to pronounced tissue degradation after mortality, A1FI sponge
336 growth could not be quantified. The fast growth observed for B1 *C. orientalis* by means of lateral
337 tissue extension around the sponge grafts (22.5 mm^2) was significantly >16 times higher than
338 those in PI (1.36 mm^2) and PD (1.08 mm^2; Fig. 4a, Table 1). However, this dramatic lateral
339 extension was not accompanied by a matching amount of $CaCO_3$ eroded by B1 *C. orientalis* over
340 the whole experimental period. Absolute amounts of sponge-eroded $CaCO_3$ remained similar
341 under all scenarios at the end of the experiment, including A1FI where total sponge mortality
342 occurred at an early stage (on average 0.26−0.37 g; Fig. 4b, Table 1). Net loss of $CaCO_3$ not
343 related to *C. orientalis* in the blank cores displayed a clear increasing trend towards A1FI

conditions (1.59%, 1.90%, 4.83% and 6.85% on average in PI, PD, B1 and A1FI, respectively; Fig. 4c, Table 1). These values represented net changes in $CaCO_3$ mass due to passive dissolution, handling, as well as the activities of residual bioeroders (e.g. endolithic algae) and calcifiers (e.g. crustose calcareous algae) that may have established in or on the coral substrate.

Discussion

Our study examined growth and survival of *C. orientalis*, as well as its responses of bioerosion and physiological parameters with respect to the symbiosis with *Symbiodinium* under four CO_2 emission scenarios. To this end, we used a more environmentally realistic approach compared to previous studies on similar topics: (1) We studied combined effects of pCO_2 and temperature in multiple scenarios, instead of independent effects of either factor, given that both factors are concurrently associated with anthropogenic CO_2 emissions (Meehl et al. 2007); (2) The computer-controlled system also administered diurnal and seasonal variability of pCO_2 and temperature as scenario offsets, resulting in close simulation of the two factors in the mesocosms as they would occur in the field (Dove et al. 2013); (3) The acclimation period and exposure period lasted 4.5 months in total, a duration which was longer than many other bioerosion experiments in the context of OA or OW (Schönberg et al. 2017a); (4) The mesocosms incorporated organismal interactions in a simulated community setting as on a local reef. Under these experimental conditions, *C. orientalis* generally displayed similar responses under PI and PD, but increasingly severe bleaching and mortality from PI to PD to B1 to A1FI.

Sponge responses and ecological consequences under A1FI

366 Under the extreme OA and OW scenario A1FI, *C. orientalis* bleached and died in the
367 mesocosms. The onset of bleaching (late November) in this community setting matched that in
368 our earlier experiment under similar A1FI conditions that only included *C. orientalis* in the tanks
369 (Fang et al. 2013a). However, Fang et al. (2013a) used a shorter post-bleaching observation
370 period (2 weeks) compared to the present study (> 2 months) and did not capture the occurrence
371 of mortality. The present results support our previous hypothesis that, under severe bleaching,
372 the loss of photoautotrophic energy formerly provided by *Symbiodinium* can lead to an
373 unsustainable carbon budget and can be lethal for *C. orientalis* (Fang et al. 2014). Along with the
374 sponge mortality, a few genera of A1FI corals also bleached and died, but some other corals
375 survived in a bleached state (Dove et al. 2013). These surviving bleached corals may be able to
376 adjust heterotrophic feeding rates to meet their metabolic demands (Grottoli et al. 2006; Dove et
377 al. 2013). However, present and previous results have not yet provided evidence for
378 heterotrophic plasticity in *C. orientalis* (Fang et al. 2014; Fang et al. 2017a). The present
379 findings imply that *C. orientalis*, one of the most dominant bioeroding sponges on the GBR
380 (Schönberg 2001 and unpubl. data), may reach physiological limits under future conditions and
381 may lose some of its competitive advantage towards live corals (see Schönberg and Wilkinson
382 2001; Achlatis et al. 2017).
383
384 A1FI *C. orientalis*, when alive, displayed the fastest bioerosion among all scenarios in our earlier
385 study (Fang et al. 2013a). However, approximately two months after the sponge mortality in the
386 present A1FI treatment, *C. orientalis* in PI and PD reached similar amounts of eroded $CaCO_3$ as
387 in A1FI (Fig. 4b). This suggests that although *C. orientalis* and other photosynthetic clionaid
388 sponges can develop a stronger bioerosion capability under A1FI, their effects on reef carbonate

budgets may only be temporary as the sponges may not survive long-term under such conditions. However, the sponges' tolerance to changing environments, their likelihood of survival and performance of bioerosion clearly depend on how they will adapt to the conditions developing over the coming decades. Although some bioeroding sponges may not survive in the future, temporary stimulation of sponge bioerosion followed by their ultimate demise may still have far reaching impacts on the structure and function of future coral reefs. First, mid-term bioerosion is still likely to increase, as changing conditions such as OA may for a while favour different guilds of bioeroders that support each other and feed back into the 'bioerosion loop' (see Schönberg et al. 2017a). Second, death and decay of bioeroding sponges would leave behind a porous reef structure, which was before covered and filled by the sponge tissue and thus to some extent more 'protected'. This porous reef structure would then be exposed and become more susceptible to re-colonisation by algae, external bioerosion by grazers (Schönberg et al. 2017a), abiotic chemical erosion (e.g. accelerating dissolution of $CaCO_3$; Fig. 4c) and physical erosion (e.g. via increasing intensity of tropical cyclones; Knutson et al. 2010).

Sponge responses and ecological consequences under B1

Under the intermediate OA and OW scenario B1, *C. orientalis* extended its surface area at rates much higher than those under PI and PD (Fig. 4a), an observation that can confirm our earlier findings in terms of organic mass (Fang et al. 2013a). The fast growth of *C. orientalis* under B1 before bleaching can be explained by the temporarily enhanced productivity of its mutualistic *Symbiodinium* (Fang et al. 2014). Given the apparent dependence of *C. orientalis* on *Symbiodinium* in its energy budget, bleaching observed in B1 may represent a tipping point for the sponge's health and survival. Sponge bleaching was confirmed by the loss of colour and by

chlorophyll fluorescence. Compared to previous near-zero values obtained from A1FI bleached *C. orientalis* with 99.5% loss of *Symbiodinium* (before mortality; Fang et al. 2013a, 2016), the values of Abs, F_o and F_v/F_m here represented severe but not complete bleaching of B1 *C. orientalis* (Fig. 2). The presence of remnant *Symbiodinium* in B1 was indicated by the greatly reduced but still detectable photosynthesis (Fig. 3), which would be undetectable in a completely bleached state as previously observed in A1FI (Fang et al. 2014). This small population of *Symbiodinium* in B1 *C. orientalis* was unlikely capable of sustaining the host's metabolic demand, as revealed by the low ratio of daily gross photosynthesis to daily respiration (calculations following Fang et al. 2014). As in A1FI, bleached *C. orientalis* in B1 apparently lacked the heterotrophic plasticity to compensate for the loss of photoautotrophic energy (Fang et al. 2014). Respiration rates of bleached B1 *C. orientalis* were about half of those in PI and PD (Fig. 3). This decline in respiration to some extent indicated a reduction of biomass in the bleached sponge with an insufficient energy budget. As a result, *C. orientalis* died in some B1 cores. The accelerated bioerosion by the not-yet-bleached *C. orientalis* under B1 in Fang et al. (2013a) may also have slowed down when bleached. At the end of the experiment, the absolute amount of $CaCO_3$ eroded by B1 *C. orientalis* did not statistically differ from those under other scenarios (Fig. 4b).

Further exposure of bleached *C. orientalis* to the B1 conditions would result in two possible outcomes. Unlike some corals that can survive in a bleached state (Dove et al. 2013), losing the energy support from *Symbiodinium* may directly lead to mortality of *C. orientalis* under B1 and to similar ecological consequences as in A1FI discussed above. Alternatively, *C. orientalis* under B1 may be able to recover, considering that many cores of *C. orientalis* have already survived

through the height of B1 summer even though they bleached. It is possible that surviving *C. orientalis* would be later repopulated by the remnant *Symbiodinium* and continue to live in other B1 seasons. In this respect, recovery from severe thermal bleaching has been observed on another *C. viridis* complex sp., *Cliona varians* (Duchassaing & Michelotti, 1864) on the Florida Keys (Hill et al. 2016 and pers. comm.). In an earlier transplantation study that supposedly caused light stress, bleached *C. varians* also regained high densities of *Symbiodinium* within three months (Hill and Wilcox 1998, as *Anthosigmella varians*). This re-established population of *Symbiodinium* in *C. varians* was acquired from the environment and was assumed to be different from the original symbiont clade. Likewise, some bleached corals are capable of switching their *Symbiodinium* to other more stress-resistant clades to facilitate survival of the hosts (e.g. Boulotte et al. 2016). For *C. orientalis*, a longer-term experiment across B1 seasons will be required to test its ability to recover from bleaching, a critical factor which will determine its likelihood of survival in the future environments.

Future projections for bioeroding sponges

In summary, we have answers to our original questions as follows: *C. orientalis* appears to maintain high rates of growth and bioerosion when being supported by a healthy population of *Symbiodinium* and the resulting contribution of photoautotrophic energy. The sponge's physiological conditions may temporarily be enhanced by elevated pCO_2 and temperature. However, bleaching of *C. orientalis* and subsequent mortality are increasingly likely under more severe or longer exposures to combined OA and OW. Our follow-up experiment studying the independent effects of pCO_2 and temperature on *C. orientalis* has suggested that the observed bleaching and associated impacts on *C. orientalis* were primarily caused by elevated temperature

(Achlatis et al. 2017; see also Wisshak et al. 2013). If anthropogenic CO_2 emissions should be reduced to a comparatively mild scenario such as B1, *C. orientalis* may stand a chance of recovering from bleaching and may survive, but this is another hypothesis that has yet to be confirmed. Regardless of its recovery potential from bleaching, the fate of *C. orientalis* will also be determined by its competitiveness against reef-building corals under future ocean conditions. Such sponge-coral interactions should be investigated, e.g. using the hybrid cores devised by Fang et al. (2017b). Present results for *C. orientalis* are relevant to other photosymbiotic clionaid sponges with similar morphological features (encrusting-endolithic growth form). Investigation on other groups of bioeroding sponges will be important to make more general projections at a community level.

Acknowledgements

The experiment was co-funded by the Great Barrier Reef Foundation (to OHG), the Australian Research Council (ARC) Centre for Excellence in Coral Reef Studies CE0561435 (to SD and OHG), ARC Linkage LP0775303 (to SD and OHG), a Queensland Smart State Fellowship (to OHG), and an International Society for Reef Studies Graduate Fellowship (to JKHF). We thank the two anonymous reviewers for their valuable comments on this article, and Aaron Chai, Giovanni Bernal Carrillo, Annamieke Van Den Heuvel and Collette Bagnato for their assistance in implementing and maintaining the experiment. We also acknowledge the technical support provided by the staff at Heron Island Research Station. All experimental cores were collected under a permit provided by the Great Barrier Reef Marine Park Authority (G10/33917.1).

References

Achlatis M, van der Zande RM, Schönberg CHL, Fang JKH, Hoegh-Guldberg O, Dove S (2017) Sponge bioerosion on changing reefs: ocean warming poses physiological constraints to the success of a photosymbiotic excavating sponge. Sci Rep 7:10705

Boulotte NM, Dalton SJ, Carroll AG, Harrison PL, Putnam HM, Peplow LM, van Oppen MJH (2016) Exploring the *Symbiodinium* rare biosphere provides evidence for symbiont switching in reef-building corals. ISME J 10:2693–2701

Calcinai B, Azzini F, Bavestrello G, Gaggero L, Cerrano C (2007) Excavating rates and boring pattern of *Cliona albimarginata* (Porifera: Clionaidae) in different substrata. In: Custódio MR, Lôbo-Hajdu G, Hajdu E, Muricy G (eds) Porifera research: biodiversity, innovation and sustainability. Série Livros 28, Museu Nacional, Rio de Janeiro, pp 203–210

Dove SG, Kline DI, Pantos O, Angly FE, Tyson GW, Hoegh-Guldberg O (2013) Future reef decalcification under a business-as-usual CO_2 emission scenario. P Natl Acad Sci USA 110:15342–15347

Enochs IC, Manzello DP, Calton RD, Graham DM, Ruzicka R, Colella MA (2015) Ocean acidification enhances the bioerosion of a common coral reef sponge: implications for the persistence of the Florida Reef Tract. B Mar Sci 91:271–290

Enochs IC, Manzello DP, Kolodziej G, Noonan SHC, Valentino L, Fabricius KE (2016) Enhanced marcoboring and depressed calcification drive net dissolution at high-CO_2 coral reefs. Proc R Soc B 283:20161742

Fang JKH, Mason RAB, Schönberg CHL, Hoegh-Guldberg O, Dove S (2017b) Studying interactions between excavating sponges and massive corals by the use of hybrid cores. Mar Ecol 38:e12393

503 Fang JKH, Mello-Athayde MA, Schönberg CHL, Kline DI, Hoegh-Guldberg O, Dove S (2013a)
504 Sponge biomass and bioerosion rates increase under ocean warming and acidification. Glob
505 Change Biol 19:3581−3591
506 Fang JKH, Schönberg CHL (2015) Carbonate budgets of coral reefs: recent developments in
507 excavating sponge research. Reef Encounter 30:43−46
508 Fang JKH, Schönberg CHL, Hoegh-Guldberg O, Dove S (2016) Day-night ecophysiology of the
509 photosymbiotic bioeroding sponge *Cliona orientalis* Thiele, 1900. Mar Biol 163:100
510 Fang JKH, Schönberg CHL, Hoegh-Guldberg O, Dove S (2017a). Symbiotic plasticity of
511 *Symbiodinium* in a common excavating sponge. Mar Biol 164:104
512 Fang JKH, Schönberg CHL, Kline DI, Hoegh-Guldberg O, Dove S (2013b) Methods to quantify
513 components of the excavating sponge *Cliona orientalis* Thiele, 1900. Mar Ecol 34:193−206
514 Fang JKH, Schönberg CHL, Mello-Athayde MA, Hoegh-Guldberg O, Dove S (2014) Effects of
515 ocean warming and acidification on the energy budget of an excavating sponge. Glob Change
516 Biol 20:1043−1054
517 Grottoli AG, Rodrigues LJ, Palardy JE (2006) Heterotrophic plasticity and resilience in bleached
518 corals. Nature 440:1186−1189
519 Hill M, Walter C, Bartels E (2016) A mass bleaching event involving clionaid sponges. Coral
520 Reefs 35:153
521 Hill M, Wilcox T (1998) Unusual mode of symbiont repopulation after bleaching in
522 *Anthosigmella varians*: acquisition of different zooxanthellae strains. Symbiosis 25:279−289
523 Jones R, Hoegh-Guldberg O, Larkum A, Schreiber U (1998) Temperature induced bleaching of
524 corals begins with impairment to the carbon dioxide fixation mechanism of zooxanthellae.
525 Plant Cell Environ 21:1219−1230

526 Knutson TR, McBride JL, Chan J, Emanuel K, Holland G, Landsea C, Held I, Kossin JP,
527 Srivastava AK, Sugi M (2010) Tropical cyclones and climate change. Nat Geosci 3:157−163
528 Kohler KE, Gill SM (2006) Coral Point Count with Excel extensions (CPCe): a visual basic
529 program for the determination of coral and substrate coverage using random point count
530 methodology. Comput Geosci 32:1259−1269
531 Marulanda-Gómez Á, López‑Victoria M, Zea S (2017) Current status of coral takeover by an
532 encrusting excavating sponge in a Caribbean reef. Mar Ecol 38:e12379
533 McElhany P (2017) CO_2 sensitivity experiments are not sufficient to show an effect of ocean
534 acidification. ICES J Mar Sci 74:926–928
535 Middlebrook R, Anthony KRN, Hoegh-Guldberg O, Dove S (2012) Thermal priming affects
536 symbiont photosynthesis but does not alter bleaching susceptibility in *Acropora millepora*. J
537 Exp Mar Biol Ecol 432:64–72
538 Meehl, GA, Stocker TF, Collins WD, Friedlingstein P, Gaye AT, Gregory JM, Kitoh A, Knutti R,
539 Murphy JM, Noda A, Raper SCB, Watterson IG, Weaver AJ, Zhao Z-C (2007) Global
540 climate projections. In: Solomon S, Qin D, Manning M, Chen Z, Marquis M, Averyt KB,
541 Tignor M, Miller HL (eds) Climate change 2007: the physical science basis. Contribution of
542 working group I to the fourth assessment report of the Intergovernmental Panel on Climate
543 Change. Cambridge University Press, Cambridge and New York, pp 747–845
544 Perry CT, Spencer T, Kench PS (2008) Carbonate budgets and reef production states: a
545 geomorphic perspective on the ecological phase-shift concept. Coral Reefs 27:853−866
546 Rogelj J, Meinshausen M, Knutti R (2012) Global warming under old and new scenarios using
547 IPCC climate sensitivity range estimates. Nat Clim Change 2:248−253

548 Rützler K (2002) Impact of crustose clionid sponges on Caribbean reef corals. Acta Geol Hisp
549 37:61−72
550 Sampayo EM, Ridgway T, Franceschinis L, Roff G, Hoegh-Guldberg O, Dove S (2016) Coral
551 symbioses under prolonged environmental change: living near tolerance range limits. Sci Rep
552 6:36271
553 Schönberg CHL (2002) Sponges of the '*Cliona viridis* complex' − a key for species
554 identification. In: Moosa MK, Soemodihardjo S, Soegiarto A, Romimohtarto K, Nontji A,
555 Soekarno, Suharsono (eds) Proceedings of the 9th International Coral Reef Symposium.
556 International Society for Reef Studies, Indonesian Ministry of Environment and Indonesian
557 Institute of Sciences, Bali, pp 295−300
558 Schönberg CHL (2001) Small-scale distribution of Australian bioeroding sponges in shallow
559 water. Ophelia 55:39−54
560 Schönberg CHL (2017) Culture, demography and biogeography of sponge science: from past
561 conferences to strategic research? Mar Ecol 38:e12416
562 Schönberg CHL, Fang JKH, Carballo JL (2017b) Bioeroding sponges and the future of coral
563 reefs. In: Bell JJ, Carballo JL (eds) Climate change, ocean acidification, and sponges.
564 Springer, Berlin-Heidelberg, pp. 179–372
565 Schönberg CHL, Fang JKH, Carreiro-Silva M, Tribollet A, Wisshak M (2017a) Bioerosion: the
566 other ocean acidification problem. ICES J Mar Sci 74:895–925
567 Schönberg CHL, Ortiz JC (2009) Is sponge bioerosion increasing? In: Riegl BM, Dodge RE (eds)
568 Proceedings of the 11th International Coral Reef Symposium. International Society for Reef
569 Studies and US National Coral Reef Institute, Ft. Lauderdale, pp 520−523

570 Schönberg CHL, Wilkinson CR (2001) Induced colonization of corals by a clionid bioeroding
571 sponge. Coral Reefs 20:69–76
572 Strehlow BW, Jorgensen D, Webster NS, Pineda MC, Duckworth A (2016) Using a thermistor
573 flowmeter with attached video camera for monitoring sponge excurrent speed and oscular
574 behaviour. PeerJ 4:e2761
575 Stubler, AD, Furman BT, Peterson BJ (2014) Effects of pCO_2 on the interaction between an
576 excavating sponge, *Cliona varians*, and a hermatypic coral, *Porites furcata*. Mar Biol
577 161:1851−1859
578 Stubler AD, Furman BT, Peterson BJ (2015) Sponge erosion under acidification and warming
579 scenarios: differential impacts on living and dead coral. Glob Change Biol 21:4006−4020
580 Van Soest, RWM, Boury-Esnault N, Hooper JNA, Rützler K, de Voogd NJ, Alvarez de Glasby
581 B, Hajdu E, Pisera AB, Manconi R, Schönberg CHL, Klautau M, Picton B, Kelly M, Vacelet
582 J, Dohrmann M, Díaz M-C, Cárdenas P, Carballo JL (2017) World Porifera database.
583 Accessed at http://www.marinespecies.org/porifera on 19 April 2017
584 Weisz JB, Massaro AJ, Ramsby BD, Hill MS (2010) Zooxanthellar symbionts shape host sponge
585 trophic status through translocation of carbon. Biol Bull 219:189−197
586 Wisshak M, Schönberg CHL, Form A, Freiwald A (2013) Effects of ocean acidification and
587 global warming on reef bioerosion − lessons from a clionaid sponge. Aqua Biol 19:111−127
588 Wisshak M, Schönberg CHL, Form A, Freiwald A (2012) Ocean acidification accelerates reef
589 bioerosion. PLOS ONE 7:e45124
590 Wisshak M, Schönberg CHL, Form A, Freiwald A (2014) Sponge bioerosion accelerated by
591 ocean acidification across species and latitudes? Helgoland Mar Res 68:253−262
592

Table 1. Results of nested analysis of variance for data reported in Fig. 2, 3 and 4 (3 cores per variable × 3 tanks × 4 treatments). All datasets were rank-transformed prior to analysis.

Variable	Source of variation	DF	SS	MS	F	P
Apparent absorptivity	Among treatments	2	1859	929.6	37.13	< 0.001
	Among tanks within treatments	6	150.2	25.04	1.965	0.125
	Within tanks	18	229.3	14.74		
Dark-acclimated minimum fluorescence yield	Among treatments	2	1123	561.4	14.79	0.005
	Among tanks within treatments	6	227.8	37.96	2.378	0.072
	Within tanks	18	287.3	15.96		
Maximum quantum yield of photosystem II	Among treatments	2	1222	610.8	24.61	0.001
	Among tanks within treatments	6	148.9	24.82	1.161	0.369
	Within tanks	18	384.7	21.37		
Dark respiration	Among treatments	2	1098	549.0	15.59	0.004
	Among tanks within treatments	6	211.3	35.22	1.929	0.131
	Within tanks	18	328.7	18.26		
Light enhanced dark respiration	Among treatments	2	1125	562.3	40.49	< 0.001
	Among tanks within treatments	6	83.33	13.89	0.581	0.741
	Within tanks	18	430.0	23.89		
Maximum net photosynthesis	Among treatments	2	1162	580.8	31.94	< 0.001
	Among tanks within treatments	6	109.1	18.19	0.891	0.522
	Within tanks	18	367.3	20.41		
Lateral tissue extension	Among treatments	2	1172	585.8	6.181	0.035
	Among tanks within treatments	6	568.7	94.78	1.499	0.234
	Within tanks	18	1138	63.22		
Absolute loss of $CaCO_3$ by the sponge	Among treatments	3	121.0	40.33	0.193	0.898
	Among tanks within treatments	8	1673	209.2	2.401	0.046
	Within tanks	24	2091	87.11		
Net loss of $CaCO_3$ in blank substrate	Among treatments	3	2670	890.0	9.810	0.005
	Among tanks within treatments	8	725.8	90.72	4.450	0.002
	Within tanks	24	489.3	20.39		

Figure legends:

Fig. 1. Three types of experimental cores, one example per type per treatment. The sponge core was a core of massive *Porites* that was fully penetrated by tissue of the bioeroding sponge *Cliona orientalis*. The mixed core included an initially clean core of calcium carbonate ($CaCO_3$) made from the skeleton of massive *Porites* on the bottom and a smaller *C. orientalis*-penetrated core attached onto it as a graft to invade the lower *Porites* core. The blank core was an initially clean core of $CaCO_3$ also made from massive *Porites*. All cores were exposed to four carbon dioxide emission scenarios, i.e. pre-industrial (PI), present-day (PD), future B1 (intermediate acidification and warming) and future A1FI (extreme acidification and warming), after a progressive acclimation period (N = 9 per core type per treatment). Photographs were taken in mid January 2012, at which time progressive damage was apparent across the four scenarios. *C. orientalis* under PI and PD displayed similar characters. All cores of *C. orientalis* bleached under B1. All cores of *C. orientalis* died under A1FI, freeing the pre-invaded substrate for colonisation by algae. All scale bars indicate 10 mm

Fig. 2. Apparent absorptivity (Abs), dark-acclimated minimum fluorescence yield (F_o) and maximum quantum yield of photosystem II (F_v/F_m) determined from *Cliona orientalis* in the sponge cores after one h dark acclimation during daytime in mid January (mean ± SEM, N = 9; dimensionless). Asterisks indicate significantly lower values of Abs, F_o and F_v/F_m in B1 ($p < 0.05$, Tukey's multiple comparison tests following nested ANOVA; see Table 1). Refer to Fig. 1 for abbreviations of the four treatments and appearance of the sponge cores

Fig. 3. Net oxygen production by *Cliona orientalis* in the sponge cores in mid January (mean ± SEM, N = 9). Negative values represent rates of dark respiration (DR) and light-enhanced dark respiration (LEDR), while positive values represent rates of maximum net photosynthesis (NP_{Max}). Asterisks indicate significantly reduced rates of DR, LEDR and NP_{Max} in B1 ($p < 0.05$, Tukey's multiple comparison tests following nested ANOVA; see Table 1). Refer to Fig. 1 for abbreviations of the four treatments and appearance of the sponge cores

Fig. 4. (a) Lateral tissue extension by *Cliona orientalis* determined in mid January, measured as an increase in sponge area around the original grafts on the mixed cores. Refer to Fig. 1 for abbreviations of the four treatments and appearance of *C. orientalis* on the mixed cores. (b) Absolute amount of calcium carbonate ($CaCO_3$) eroded by *C. orientalis* in the same mixed cores determined over the whole experiment (1.5-month acclimation + 3-month full exposure). The results in (b) have been corrected by (c) the percentage net losses of $CaCO_3$ in the corresponding blank cores, which represent the background net changes in $CaCO_3$ mass unrelated to *C. orientalis* (mean ± SEM, N = 9). Different italic letters in (a) and (c) indicate significant differences among treatments ($p < 0.05$, Tukey's multiple comparison tests following nested ANOVA; see Table 1)

Figure 1

Click here to download Figure 2018-02-07 Figure 1.eps

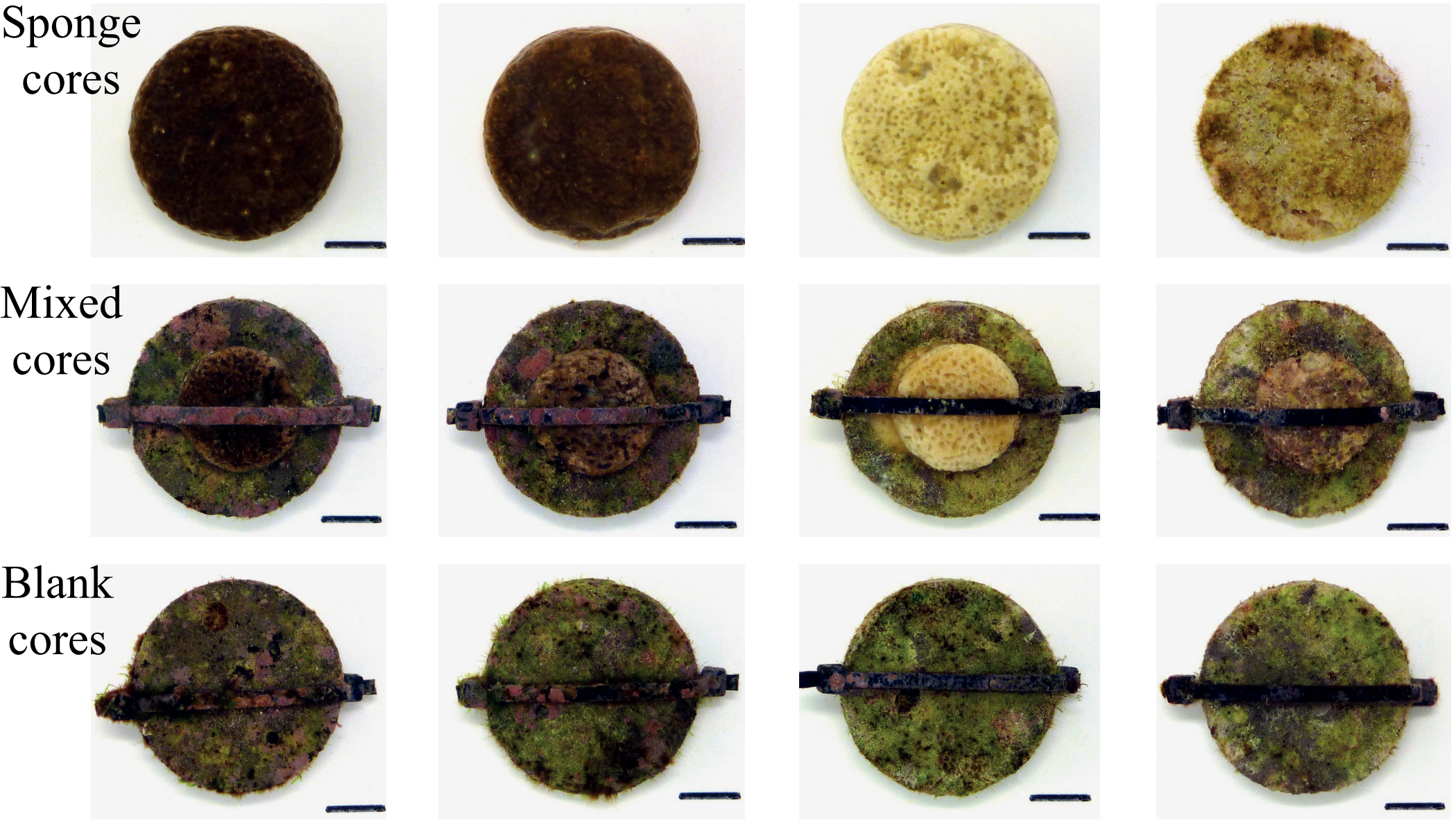

Figure 2

Click here to download Figure 2018-02-07 Figure 2.eps

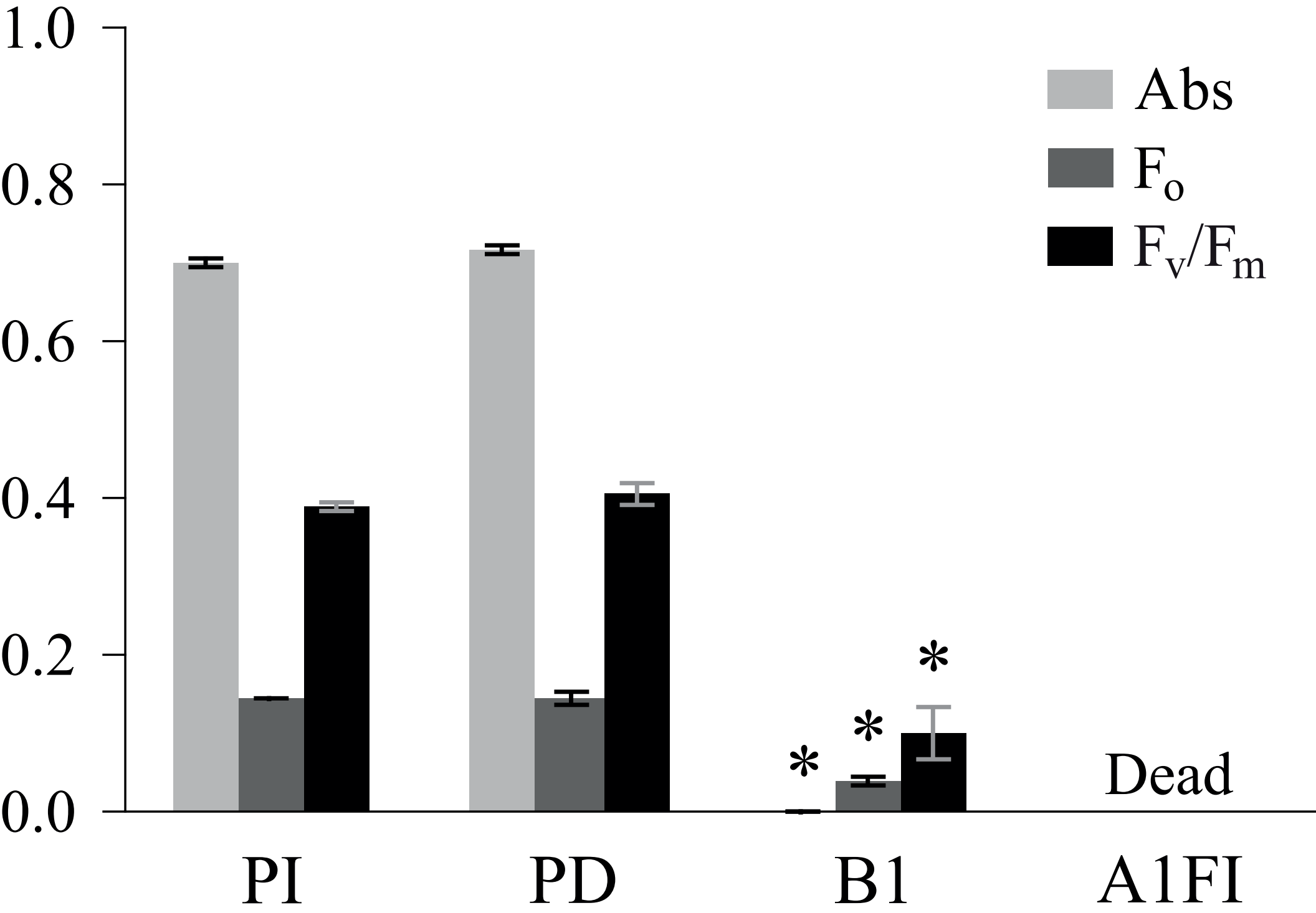

Figure 3

Click here to download Figure 2018-02-07 Figure 3.eps

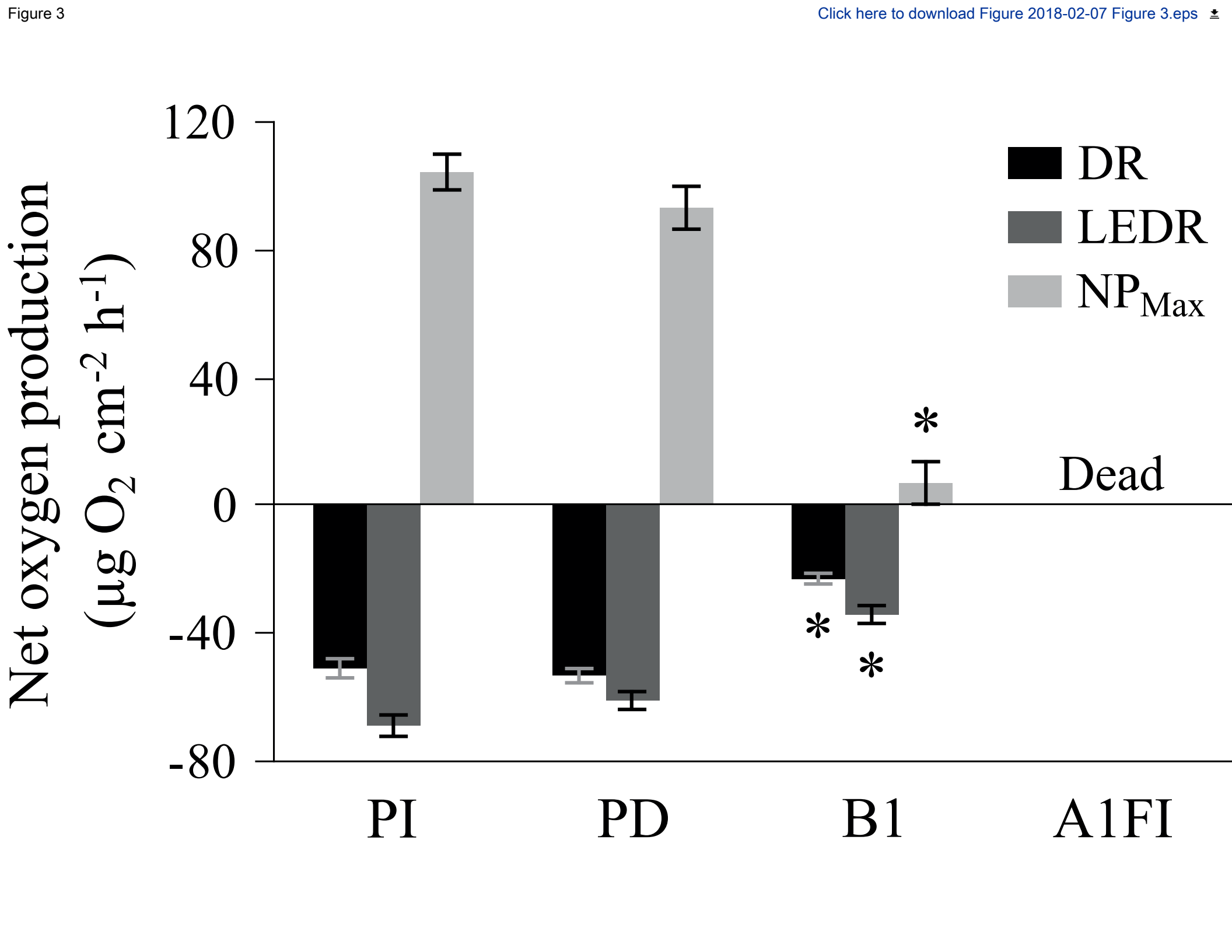

Figure 4

Click here to download Figure 2018-02-07 Figure 4.eps